Supplement of Atmos. Chem. Phys., 25, 14237–14249, 2025
https://doi.org/10.5194/acp-25-14237-2025-supplement

Atmospheric Chemistry and Physics Open Access

Supplement of

Mechanistic insights into nitric acid-enhanced iodic acid particle nucleation in the upper troposphere and lower stratosphere

Jing Li et al.

Correspondence to: An Ning (anning@bit.edu.cn) and Xiuhui Zhang (zhangxiuhui@bit.edu.cn)

Table of Contents

Supplementary Methods

^{4} s^{-1}, [IA] = 10^5 – 10^6, [NA] = 10^8 – 10^{10}, and [NH_3] = 3 × 10^8 molec. cm^{-3}.

Figure S7. Cluster formation rate J (cm^{-3} s^{-1}) as a function of [IA] or [SA] of IA–NA–NH_3 and SA–NA–NH_3 system at T = 220 K, CS = 10^{-4} s^{-1}, [IA] (or [SA]) = 10^5 – 10^6 molec. cm^{-3}, [NA] = 10^{10} molec. cm^{-3}, and [NH_3] = 3 × 10^8 molec. cm^{-3}.

Figure S8. Main cluster formation pathways of the IA–NA–NH_3 system at T = 240 K, CS = 10^{-4} s^{-1}, [IA] = 10^6 molec. cm^{-3}, [NA] = 10^9 molec. cm^{-3}, and [NH_3] = 5.5 × 10^8 molec. cm^{-3}.

Table S1. The Gibbs formation free energies ΔG_{ref} (kcal mol^{-1}) of the studied IA–NA–NH_3 clusters at the DLPNO-CCSD(T)/aug-cc-pVTZ(-PP)//ωB97X-D/6-311++G(3df,3pd) (for H, O, and N atoms) + aug-cc-pVTZ-PP with ECP28MDF (for I atom) level of theory, P = 1 atm, and T = 210, 220, 230, 240, and 260 K.

Table S2. The total evaporation rate coefficients ($\Sigma\gamma$, s^{-1}) of IA–NA–NH_3 clusters calculated at 220 – 260 K.

Table S3. Boundary conditions of the ACDC simulations at 220, 240, and 260 K, respectively.

Table S4. The Gibbs formation free energies ΔG_{ref} (kcal mol^{-1}) of the IA–NA–NH_3 and SA–NA–NH_3 systems at the DLPNO-CCSD(T)/aug-cc-pVTZ(-PP)//ωB97X-D/6-311++G(3df,3pd) (for H, O, and N atoms) + aug-cc-pVTZ-PP with ECP28MDF (for I atom) level of theory, P = 1 atm, and T = 220 K.

Table S5. The total evaporation rate coefficients ($\Sigma\gamma$, s^{-1}) of SA–NA–NH_3 clusters calculated at 220 – 260 K.

Table S6. Cartesian coordinates of all IA–NA–NH_3 clusters in the present study at the ωB97X-D/6-311++G(3df,3pd) (for H, O, and N atoms) + aug-cc-pVTZ-PP with ECP28MDF (for I atom) level of theory.

Table S7. Structural *RMSD* (in Å) and Gibbs free energy (in kcal mol^{-1}) comparisons of $(IA)_1(NA)_1$, $(IA)_1(NH_3)_1$, and $(IA)_1(NA)_1(NH_3)_1$ clusters at different levels of theory.

Supplementary Methods

Multi-step cluster conformational searching method.

First, the artificial bee colony algorithm combined with UFF force field (Rappé et al., 1992) was employed to yield more than 5000 configurations for each cluster by ABCluster (Zhang and Dolg, 2015). Then up to 1000 relatively stable structures were selected to pre-optimize at PM7 method (Stewart, 2013) by MOPAC 2016 (Stewart, 2016). Next, up to 100 low-energy ones were re-optimized with at the ωB97X-D/6-31+G* (for H, O, and N atoms) + Lanl2DZ (for I atom) level of theory (Elm and Kristensen, 2017), due to best performance of ωB97X-D functional in studying atmospheric clusters. Finally, the top 10 isomers with the low energy were optimized at ωB97X-D/6-311++G(3df,3pd) (for H, O, and N atoms) + aug-cc-pVTZ-PP with ECP28MDF (for I atom) level of theory (Francl et al., 1982; Peterson et al., 2003) to obtain the global minimum one.

Spin-orbit coupling (SOC) correction energy calculation

The spin-orbit coupling (SOC) correction energies for all iodine-containing clusters were calculated using the Gaussian 16 software (Frisch et al., 2016), which supports two-component relativistic DFT calculations. SOC effects arising from iodine were accounted for using the dhf-TZVP-2c basis set. The SOC contribution to the binding energy of each IA-containing cluster, defined as ΔE_{SOC}, was calculated as follows:

$$\Delta E_{SOC} = E_2 - E_1$$

where E_2 and E_1 represent the single-point energies calculated with and without spin-orbit potential, respectively. E_1 was calculated at the ωB97X-D/6-311++G(3df,3pd) (for H, O, and N atoms) + dhf-TZVP-2c (for I atom) level of theory. E_2 was performed by adding the "g" keyword to the method (i.e., at the gωB97X-D level). Accordingly, the ΔE_{SOC} term represents the energy difference resulting from the inclusion or exclusion of SOC effects.

The equations in Atmospheric Cluster Dynamics Code (ACDC).

The collision rate coefficient between clusters *i* and *j* ($\beta_{i,j}$) is obtained based on the kinetic gas theory, which is given as:

$$\beta_{i,j} = \left(\frac{3}{4\pi}\right)^{1/6} \left(\frac{6k_BT}{m_i} + \frac{6k_BT}{m_j}\right)^{1/2} \left(V_i^{1/3} + V_j^{1/3}\right)^2, \quad \text{(S1)}$$

where m_i and V_i are the mass and volume of cluster *i*, respectively. Equation (1) is derived from the hard-sphere collision theory where the volume of molecule clusters $V_i = 3/4 \times \pi \times (d_i/2)^3$. The diameter d_i of cluster *i* is derived from the cluster volume V_i calculated by Multiwfn 3.7 (Lu and Chen, 2012). Evaporation rate coefficient $\gamma_{(i+j)\to i}$ is derived from the collision coefficients based on the detailed balance assumption:

$$\gamma_{(i+j)\to i} = \beta_{i,j} \frac{P_{\text{ref}}}{k_BT} \exp\left(\frac{\Delta G_{i+j} - \Delta G_i - \Delta G_j}{k_BT}\right), \quad \text{(S2)}$$

where P_{ref} is the reference pressure (1 atm) and ΔG_i is the Gibbs free energy of the formation of cluster *i*.

Boundary setting in ACDC simulation.

In general, a lower evaporation rate translates into a higher cluster stability. Table S2 display the total evaporation rates ($\Sigma\gamma$, s^{-1}) of IA–NA–NH_3 clusters at temperatures ranging from 220 to 260 K. In ACDC simulations, the stability of clusters within the simulated system depends on the ratio of collision frequencies between the clusters and monomer molecule at the concentration *C* to the total evaporation frequencies of clusters ($\beta C/\Sigma\gamma$). If $\beta C/\Sigma\gamma$ of a cluster is greater than 1, the cluster is stable and may continue to grow. In this study, we systematically considered the collisions involving all monomer species, namely IA, NA, and NH_3. The boundary cluster settings for the system at different temperatures (220 – 260 K) are shown in Table S3.

Benchmarks.

To confirm that the structures of the most stable clusters optimized at ωB97X-D/6-311++G(3df,3pd) (for H, O, and N atoms) + aug-cc-pVTZ-PP (for I atom) level of theory are reasonable, three clusters ($(IA)_1(NA)_1$, $(IA)_1(NH_3)_1$, and $(IA)_1(NA)_1(NH_3)_1$) were optimized by ωB97X-D functional with 6-311++G(3df,3pd) (for H, O, and N atoms) + aug-cc-pVTZ-PP (for I atom) and aug-cc-pVTZ (for H, O, and N atoms) + aug-cc-pVTZ-PP (for I atom) basis sets. And the optimized cluster structures with different basis sets were compared by calculating the root-mean-square deviations (*RMSD*, the index of the difference between the two structures, is calculated as Eq. (S3)).

$$RMSD = \sqrt{\frac{1}{N}\sum_{i}^{n}[(x_i - x_i^{'})^2 + (y_i - y_i^{'})^2 + (z_i - z_i^{'})^2]} \quad \text{(S3)}$$

where (x_i, y_i, z_i) and (x_i', y_i', z_i') are the coordinates of the atom i of two structures optimized with two different basis sets, respectively. As shown in Table S7, the *RMSD* between the structures of any one of three clusters are lower than 0.1 Å, indicating that the differences among structures of clusters optimized with two different basis sets are negligible.

Besides, to test the effects of the chosen basis set on the Gibbs free energy of cluster formation (ΔG, kcal mol^{-1}), the optimizations and frequencies calculations of $(IA)_1(NA)_1$, $(IA)_1(NH_3)_1$, and $(IA)_1(NA)_1(NH_3)_1$ clusters were performed by ωB97X-D functional using 6-311++G(3df,3pd) (for H, O, and N atoms) + aug-cc-pVTZ-PP (for I atom) and aug-cc-pVTZ (for H, O, and N atoms) + aug-cc-pVTZ-PP (for I atom) basis sets, respectively. The final Gibbs free energies are calculated by Eq. (S4):

$$\Delta G_{\text{DLPNO-CCSD(T)}} = \Delta G_{\text{thermal}}^{\omega\text{B97X-D}} + \Delta E_{\text{DLPNO-CCSD(T)}}, \quad \text{(S4)}$$

The thermal contributions ($\Delta G_{\text{thermal}}^{\omega\text{B97X-D}}$) were obtained from calculations using two different basis sets. Subsequently, the single-point energies ($\Delta E_{\text{DLPNO-CCSD(T)}}$) of the corresponding optimized clusters were calculated at the DLPNO-CCSD(T)/aug-cc-pVTZ(-PP) level of theory. The final Gibbs free energies ($\Delta G_{\text{DLPNO-CCSD(T)}}$) were derived by combining the thermal contributions with the single-point energies, and the differences between the two basis sets ($\Delta\Delta G_{\text{DLPNO-CCSD(T)}}$) were then evaluated. Furthermore, to assess the accuracy of the DLPNO-CCSD(T) method employed for single-point energy calculations, a comparison was conducted against the results obtained using the

more accurate CCSD(T) method. Here, $\Delta G_{CCSD(T)}$ denotes the energy calculated at the CCSD(T)/aug-cc-pVTZ(-PP)//ωB97X-D/6-311++G(3df,3pd) (for H, O, and N atoms) + aug-cc-pVTZ-PP (for I atom) level of theory. As presented in Table S7, the $\Delta\Delta G$ values for the three clusters are less than 1 kcal mol^{-1}, suggesting that the differences in the calculated Gibbs free energies obtained using the two basis sets, i.e., 6-311++G(3df,3pd) (for H, O, and N atoms) + aug-cc-pVTZ-pp (for I atom) and aug-cc-pVTZ (for H, O, and N atoms) + aug-cc-pVTZ-PP (for I atom), are minimal. Moreover, the energy differences after the correction of DLPNO-CCSD(T) and CCSD(T) methods are also minor, suggesting that the DLPNO-CCSD(T) method provides sufficiently reliable results compared to the "gold standard" CCSD(T) results.

In summary, these benchmarks sufficiently proved the reliability of methods used in this study, and therefore the results and conclusions of our study are reliable and convincing.

Enhancement of NA on nucleation.

Despite the identified NA's effective role in IA nucleation, the specific strength, particularly across a broader range of atmospheric conditions, remains unclear. Herein, we have calculated the enhancement strength *R* (Eq. (S5)) to quantify the rate enhancement of IA–NA–NH_3 ternary nucleation on IA–NH_3 and NA–NH_3 binary nucleation.

$$R = \frac{J\left(\left[\mathrm{IA}\right]=10^6,\left[\mathrm{NA}\right]=x,\left[\mathrm{NH_3}\right]=y\right)}{J\left(\left[\mathrm{IA}\right]=10^6,\left[\mathrm{NA}\right]=0,\left[\mathrm{NH_3}\right]=y\right)+J\left(\left[\mathrm{IA}\right]=0,\left[\mathrm{NA}\right]=x,\left[\mathrm{NH_3}\right]=y\right)}, \quad \text{(S5)}$$

where *J* denotes the cluster formation rate. Due to the potentially low concentration of IA in the UTLS and the lack of available field measurement, here the [IA] is set to a lower value of 10^6 molec. cm^{-3}. *R* is shown in Fig. S5 as a function of [NA].

As expected, NH_3 level is a key factor influencing *R* due to the vital base-stabilization on both acidic NA and IA. Additionally, *R* is sensitive to temperature variation, showing a negative correlation. At low temperatures, entropy effects are decreased, and all cluster formation free energies are more negative (Bork et al., 2014), resulting in more stable clusters and a higher *R*. At high NH_3 levels, NH_3 is in large excess compared to IA, and the growth of clusters is thus limited by acid collisions. Consequently, the introduction of an additional acid source, such as increased NA concentrations, would have a more significant impact. When the [NA] is below 10^{10} molec. cm^{-3}, its variation exerts a minimal impact on changes in *R*. However, once [NA] exceeds 10^{10} molec. cm^{-3}, further increases in [NA] can enhance *J* by up to 120%. Overall, the role of IA–NA–NH_3 system is stronger in regions with lower temperatures and higher concentrations of NA and NH_3, which corresponds to the real environmental conditions in the UTLS.

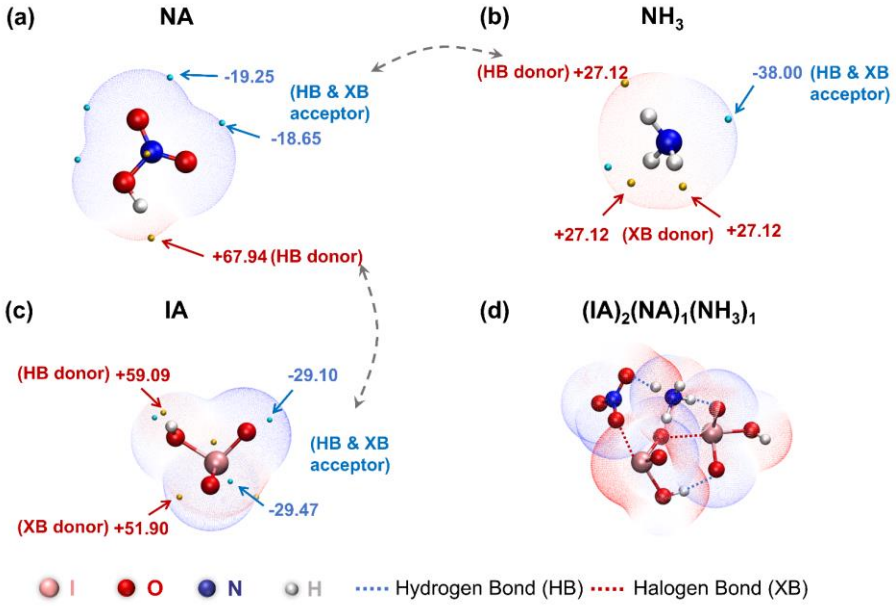

Figure S1. The ESP-mapped molecular vdW surface of **(a)** NA, **(b)** NH_3, **(c)** IA, and **(d)** $(IA)_2(NA)_1(NH_3)_1$. The golden and cyan dots represent the positions of maximums and minimums of ESP (unit: kcal mol^{-1}), respectively. The gray dashed arrows signify the site-to-site interaction tendencies.

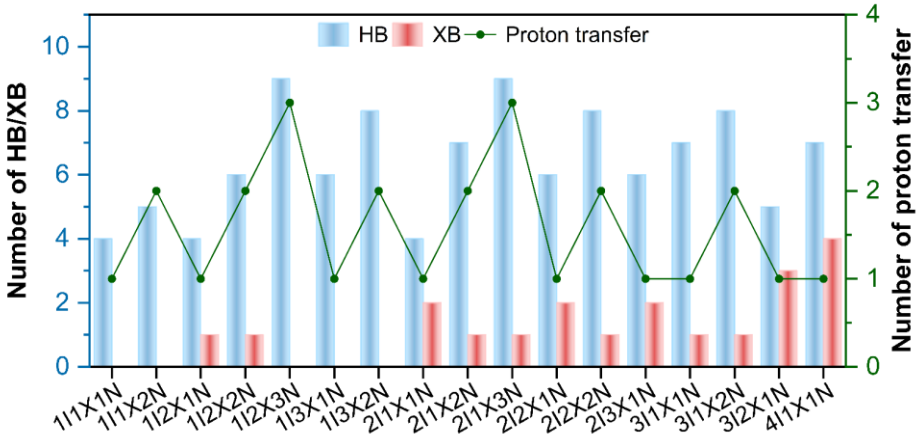

Figure S2. The number of hydrogen bonds (HB), halogen bonds (XB), and proton transfers in the IA–NA–NH_3 clusters, where I represents iodic acid (IA), X represents nitric acid (NA), and N represents ammonia (NH_3).

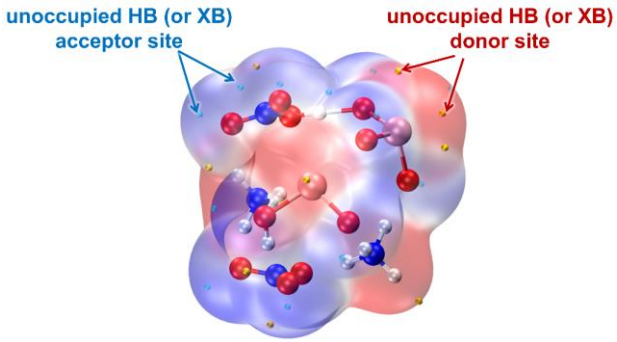

Figure S3. The ESP-mapped molecular vdW surfaces of the $(IA)_2(NA)_2(NH_3)_2$ cluster. The red region is the electron-deficient region, and the blue region is the electron-rich region.

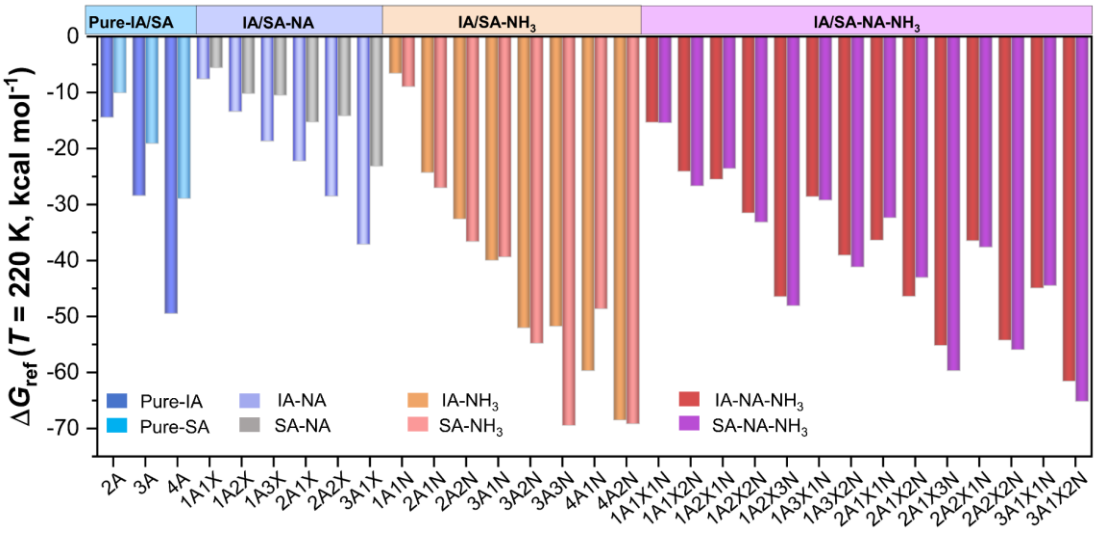

Figure S4. The Gibbs free energy (ΔG_{ref}, kcal mol^{-1}) of IA–NA–NH_3 and SA–NA–NH_3 system at T = 220 K, where A represents iodic acid (IA) or sulfuric acid (SA), X represents nitric acid (NA), and N represents ammonia (NH_3).

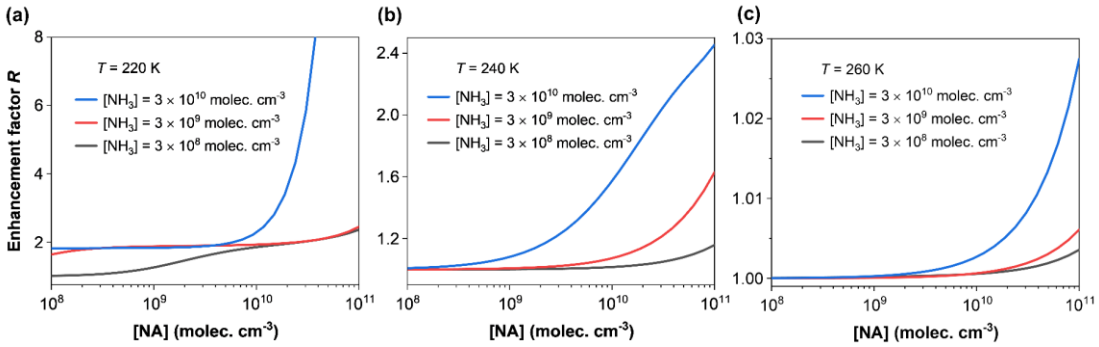

Figure S5. Enhancement strength (R) of IA–NA–NH_3 nucleation. The ACDC simulations were performed at the conditions of CS = 10^{-4} s^{-1}, [IA] = 10^6 molec. cm^{-3}, [NH_3] = 3 × 10^8 – 3 × 10^{10} molec. cm^{-3}, **(a)** T = 220 K, **(b)** T = 240 K, and **(c)** T = 260 K.

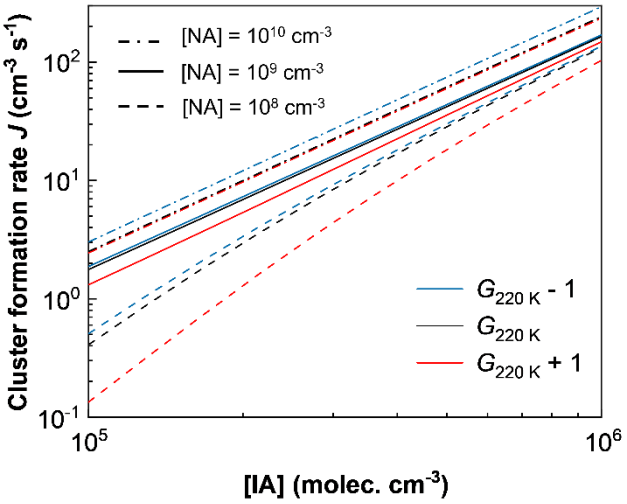

Figure S6. Cluster formation rate J as a function of [IA] = 10^5 – 10^6 molec. cm^{-3}, with different energy of ΔG_{220K} (black line), ΔG_{220K} – 1 (blue line), ΔG_{220K} + 1 (red line), at T = 220 K, CS = 10^{-4} s^{-1}, [IA] = 10^5 – 10^6, [NA] = 10^8 – 10^{10}, and [NH_3] = 3 × 10^8 molec. cm^{-3}.

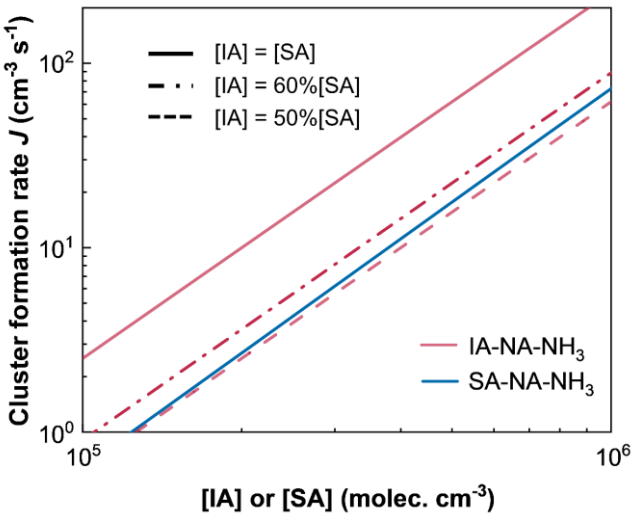

Figure S7. Cluster formation rate J (cm^{-3} s^{-1}) as a function of [IA] or [SA] of IA–NA–NH_3 and SA–NA–NH_3 system at T = 220 K, CS = 10^{-4} s^{-1}, [IA] (or [SA]) = 10^5 – 10^6 molec. cm^{-3}, [NA] = 10^{10} molec. cm^{-3}, and [NH_3] = 3 × 10^8 molec. cm^{-3}.

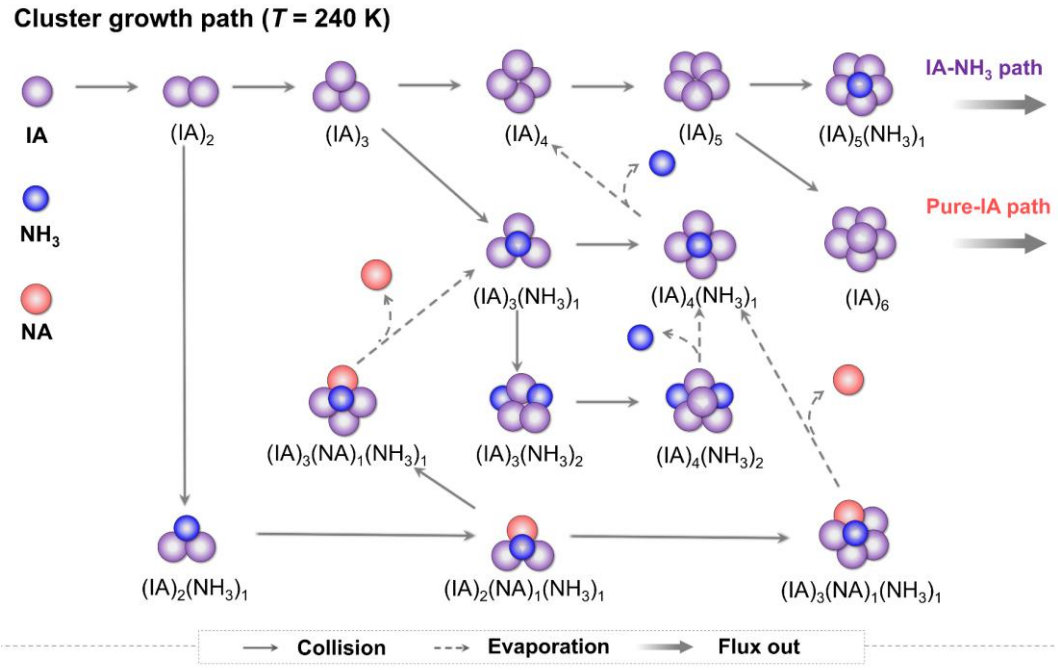

Figure S8. Main cluster formation pathways of the IA–NA–NH_3 system at T = 240 K, CS = 10^{-4} s^{-1}, [IA] = 10^6 molec. cm^{-3}, [NA] = 10^9 molec. cm^{-3}, and [NH_3] = 5.5 × 10^8 molec. cm^{-3}.

Table S1. The Gibbs formation free energies ΔG_{ref} (kcal mol^{-1}) of the studied IA–NA–NH_3 clusters at the DLPNO-CCSD(T)/aug-cc-pVTZ(-PP)//ωB97X-D/6-311++G(3df,3pd) (for H, O, and N atoms) + aug-cc-pVTZ-PP with ECP28MDF (for I atom) level of theory, P = 1 atm, and T = 210, 220, 230, 240, and 260 K.

Clusters	ΔG (kcal mol^{-1})				
	210K	**220K**	**230K**	**240K**	**260K**
$(IA)_1(NA)_1$	-7.91	-7.57	-7.22	-6.88	-6.20
$(IA)_1(NA)_2$	-14.11	-13.38	-12.65	-11.93	-10.48
$(IA)_1(NA)_3$	-19.71	-18.65	-17.59	-16.54	-14.44
$(IA)_2(NA)_1$	-22.94	-22.22	-21.51	-20.80	-19.39
$(IA)_2(NA)_2$	-29.66	-28.50	-27.35	-26.21	-23.93
$(IA)_2(NA)_3$	-35.89	-34.38	-32.87	-31.36	-28.37
$(IA)_3(NA)_1$	-38.31	-37.09	-35.89	-34.69	-32.30
$(IA)_3(NA)_2$	-45.94	-44.39	-42.83	-41.29	-38.22
$(IA)_3(NA)_3$	-51.80	-49.88	-47.96	-46.05	-42.24
$(IA)_4(NA)_1$	-54.55	-52.98	-51.41	-49.86	-46.76
$(IA)_4(NA)_2$	-64.53	-62.50	-60.47	-58.46	-54.45
$(NA)_2$	-2.12	-1.77	-1.42	-1.07	-0.36
$(NA)_3$	-0.71	-0.02	0.67	1.35	2.71
$(IA)_2$	-14.79	-14.41	-14.02	-13.64	-12.89
$(IA)_3$	-29.22	-28.40	-27.59	-26.79	-25.19
$(IA)_4$	-50.71	-49.46	-48.21	-46.97	-44.50
$(IA)_5$	-69.38	-67.70	-66.02	-64.35	-61.02
$(IA)_6$	-87.32	-85.18	-83.05	-80.94	-76.73
$(IA)_1(NH_3)_1$	-6.82	-6.55	-6.28	-6.02	-5.50
$(IA)_1(NH_3)_2$	-11.38	-10.72	-10.06	-9.40	-8.07
$(IA)_1(NH_3)_3$	-16.40	-15.46	-14.50	-13.56	-11.66
$(IA)_2(NH_3)_1$	-25.00	-24.26	-23.52	-22.78	-21.31
$(IA)_2(NH_3)_2$	-33.62	-32.55	-31.48	-30.41	-28.28
$(IA)_2(NH_3)_3$	-33.56	-32.21	-30.86	-29.51	-26.82
$(IA)_3(NH_3)_1$	-41.08	-39.94	-38.79	-37.65	-35.38
$(IA)_3(NH_3)_2$	-53.57	-52.02	-50.47	-48.92	-45.84
$(IA)_3(NH_3)_3$	-53.51	-51.71	-49.92	-48.13	-44.58
$(IA)_4(NH_3)_1$	-61.23	-59.67	-58.11	-56.56	-53.48

$(IA)_4(NH_3)_2$	-70.44	-68.49	-66.54	-64.60	-60.73
$(IA)_5(NH_3)_1$	-81.43	-79.36	-77.29	-75.24	-71.14
$(NH_3)_2$	2.29	2.51	2.72	2.94	3.38
$(NH_3)_3$	3.14	3.66	4.18	4.70	5.73
$(NA)_1(NH_3)_1$	-6.21	-5.92	-5.63	-5.35	-4.78
$(NA)_2(NH_3)_1$	-8.97	-8.36	-7.75	-7.13	-5.92
$(NA)_2(NH_3)_2$	-16.71	-15.66	-14.61	-13.55	-11.46
$(NA)_3(NH_3)_1$	-13.71	-12.71	-11.71	-10.71	-8.72
$(NA)_3(NH_3)_2$	-24.94	-23.58	-22.21	-20.85	-18.13
$(NA)_3(NH_3)_3$	-33.24	-31.48	-29.72	-27.96	-24.45
$(NA)_4(NH_3)_1$	-17.88	-16.43	-14.98	-13.53	-10.64
$(NA)_4(NH_3)_2$	-30.24	-28.48	-26.73	-24.98	-21.49
$(NA)_5(NH_3)_1$	-21.73	-19.90	-18.07	-16.25	-12.63
$(IA)_1(NA)_1(NH_3)_1$	-15.99	-15.29	-14.58	-13.88	-12.47
$(IA)_1(NA)_1(NH_3)_2$	-25.08	-24.05	-23.01	-21.98	-19.91
$(IA)_2(NA)_1(NH_3)_1$	-37.52	-36.35	-35.18	-34.02	-31.71
$(IA)_2(NA)_1(NH_3)_2$	-47.94	-46.38	-44.81	-43.25	-40.13
$(IA)_2(NA)_1(NH_3)_3$	-57.00	-55.16	-53.32	-51.48	-47.82
$(IA)_3(NA)_1(NH_3)_1$	-46.36	-44.89	-43.43	-41.97	-39.06
$(IA)_3(NA)_1(NH_3)_2$	-63.43	-61.53	-59.63	-57.73	-53.95
$(IA)_4(NA)_1(NH_3)_1$	-71.39	-69.35	-67.31	-65.28	-61.23
$(IA)_1(NA)_2(NH_3)_1$	-26.54	-25.46	-24.37	-23.29	-21.13
$(IA)_1(NA)_2(NH_3)_2$	-32.99	-31.48	-29.97	-28.46	-25.46
$(IA)_1(NA)_2(NH_3)_3$	-48.27	-46.42	-44.56	-42.71	-39.02
$(IA)_2(NA)_2(NH_3)_1$	-38.02	-36.46	-34.89	-33.32	-30.21
$(IA)_2(NA)_2(NH_3)_2$	-56.17	-54.20	-52.23	-50.27	-46.35
$(IA)_3(NA)_2(NH_3)_1$	-57.29	-55.32	-53.35	-51.38	-47.47
$(IA)_1(NA)_3(NH_3)_1$	-30.08	-28.56	-27.05	-25.53	-22.52
$(IA)_1(NA)_3(NH_3)_2$	-40.88	-39.04	-37.21	-35.37	-31.72
$(IA)_2(NA)_3(NH_3)_1$	-45.39	-43.50	-41.62	-39.75	-36.02

Table S2. The total evaporation rate coefficients ($\Sigma\gamma$, s^{-1}) of IA–NA–NH_3 clusters calculated at 220 – 260 K.

Clusters	$\Sigma\gamma$ (s^{-1})		
	220 K	**240 K**	**260 K**
$(IA)_2$	1.77×10^{-5}	1.33×10^{-3}	4.91×10^{-2}
$(IA)_3$	9.97×10^{-5}	8.00×10^{-3}	3.32×10^{-1}
$(IA)_4$	1.03×10^{-11}	3.47×10^{-9}	4.65×10^{-7}
$(IA)_5$	7.04×10^{-9}	1.32×10^{-6}	1.11×10^{-4}
$(IA)_6$	4.27×10^{-8}	7.39×10^{-6}	5.66×10^{-4}
$(NA)_2$	8.30×10^{7}	4.83×10^{8}	2.18×10^{9}
$(NA)_3$	5.65×10^{11}	1.58×10^{12}	3.62×10^{12}
$(NH_3)_2$	2.01×10^{12}	2.94×10^{12}	4.12×10^{12}
$(NH_3)_3$	1.97×10^{11}	5.45×10^{11}	1.23×10^{12}
$(IA)_1(NA)_1$	5.38×10^{2}	9.27×10^{3}	1.01×10^{5}
$(IA)_1(NA)_2$	1.73×10^{4}	2.47×10^{5}	2.38×10^{6}
$(IA)_1(NA)_3$	6.58×10^{4}	6.87×10^{5}	4.88×10^{6}
$(IA)_2(NA)_1$	1.83×10^{2}	3.03×10^{3}	3.31×10^{4}
$(IA)_2(NA)_2$	6.68×10^{3}	1.31×10^{5}	1.62×10^{6}
$(IA)_2(NA)_3$	1.80×10^{4}	2.44×10^{5}	2.13×10^{6}
$(IA)_3(NA)_1$	2.78×10^{1}	7.31×10^{2}	1.16×10^{4}
$(IA)_3(NA)_2$	7.18×10^{2}	1.20×10^{4}	1.25×10^{5}
$(IA)_3(NA)_3$	4.83×10^{4}	6.08×10^{5}	5.27×10^{6}
$(IA)_4(NA)_1$	4.19×10^{6}	2.94×10^{7}	1.52×10^{8}
$(IA)_4(NA)_2$	4.88×10^{0}	1.98×10^{2}	4.42×10^{3}
$(IA)_1(NH_3)_1$	8.20×10^{3}	8.32×10^{4}	5.77×10^{5}
$(IA)_1(NH_3)_2$	1.07×10^{6}	1.19×10^{7}	9.46×10^{7}
$(IA)_1(NH_3)_3$	3.13×10^{5}	2.50×10^{6}	1.41×10^{7}
$(IA)_2(NH_3)_1$	2.72×10^{0}	7.53×10^{1}	1.27×10^{3}
$(IA)_2(NH_3)_2$	1.03×10^{2}	1.90×10^{3}	2.25×10^{4}
$(IA)_2(NH_3)_3$	4.09×10^{10}	1.19×10^{11}	2.91×10^{11}
$(IA)_3(NH_3)_1$	6.66×10^{-2}	2.40×10^{0}	4.85×10^{1}
$(IA)_3(NH_3)_2$	2.04×10^{-2}	1.07×10^{0}	3.02×10^{1}

$(IA)_3(NH_3)_3$	4.30×10^{10}	1.06×10^{11}	2.23×10^{11}
$(IA)_4(NH_3)_1$	1.57×10^{0}	3.85×10^{1}	5.66×10^{2}
$(IA)_4(NH_3)_2$	3.94×10^{1}	1.04×10^{3}	1.69×10^{4}
$(IA)_5(NH_3)_1$	6.22×10^{-2}	2.76×10^{0}	6.82×10^{1}
$(NA)_1(NH_3)_1$	3.25×10^{4}	3.18×10^{5}	2.18×10^{6}
$(NA)_2(NH_3)_1$	3.91×10^{7}	2.38×10^{8}	1.05×10^{9}
$(NA)_2(NH_3)_2$	9.12×10^{2}	2.22×10^{4}	3.30×10^{5}
$(NA)_3(NH_3)_1$	5.28×10^{5}	5.83×10^{6}	4.51×10^{7}
$(NA)_3(NH_3)_2$	1.57×10^{2}	2.51×10^{3}	2.66×10^{4}
$(NA)_3(NH_3)_3$	2.73×10^{0}	6.19×10^{3}	8.63×10^{4}
$(NA)_4(NH_3)_1$	2.40×10^{6}	3.08×10^{7}	2.66×10^{8}
$(NA)_4(NH_3)_2$	1.69×10^{5}	2.07×10^{6}	1.72×10^{7}
$(NA)_5(NH_3)_1$	4.55×10^{6}	4.06×10^{7}	2.49×10^{8}
$(IA)_1(NA)_1(NH_3)_1$	3.62×10^{2}	7.16×10^{3}	9.30×10^{4}
$(IA)_1(NA)_1(NH_3)_2$	3.35×10^{1}	6.80×10^{2}	8.65×10^{3}
$(IA)_2(NA)_1(NH_3)_1$	1.10×10^{-2}	6.35×10^{-1}	1.93×10^{1}
$(IA)_2(NA)_1(NH_3)_2$	2.12×10^{0}	7.33×10^{1}	1.50×10^{3}
$(IA)_2(NA)_1(NH_3)_3$	3.86×10^{1}	6.25×10^{2}	6.44×10^{3}
$(IA)_3(NA)_1(NH_3)_1$	1.51×10^{5}	1.40×10^{6}	9.31×10^{6}
$(IA)_3(NA)_1(NH_3)_2$	4.62×10^{0}	1.18×10^{2}	1.81×10^{3}
$(IA)_4(NA)_1(NH_3)_1$	3.33×10^{0}	1.51×10^{2}	3.87×10^{3}
$(IA)_1(NA)_2(NH_3)_1$	8.77×10^{-1}	2.89×10^{1}	5.45×10^{2}
$(IA)_1(NA)_2(NH_3)_2$	2.02×10^{4}	3.67×10^{5}	4.19×10^{6}
$(IA)_1(NA)_2(NH_3)_3$	2.83×10^{-5}	1.98×10^{-3}	7.22×10^{-2}
$(IA)_2(NA)_2(NH_3)_1$	9.38×10^{9}	5.01×10^{10}	2.02×10^{11}
$(IA)_2(NA)_2(NH_3)_2$	2.14×10^{2}	4.88×10^{3}	6.84×10^{4}
$(IA)_3(NA)_2(NH_3)_1$	8.96×10^{-1}	4.86×10^{1}	1.40×10^{3}
$(IA)_1(NA)_3(NH_3)_1$	9.88×10^{6}	1.04×10^{8}	7.41×10^{8}
$(IA)_1(NA)_3(NH_3)_2$	3.82×10^{2}	6.04×10^{3}	6.24×10^{4}
$(IA)_2(NA)_3(NH_3)_1$	1.33×10^{3}	1.78×10^{4}	1.63×10^{5}

Table S3. Boundary conditions of the ACDC simulations at 220 K, 240 K, and 260 K, respectively.

Temperature (K)	Boundary cluster
220 K	$(IA)_7$
	$(IA)_6(NA)_1$
	$(IA)_6(NH_3)_1$
	$(IA)_5(NH_3)_2$
	$(IA)_2(NA)_2(NH_3)_3$
	$(IA)_5(NA)_1(NH_3)_1$
	$(IA)_1(NA)_3(NH_3)_3$
240 K	$(IA)_7$
	$(IA)_6(NA)_1$
	$(IA)_6(NH_3)_1$
	$(IA)_1(NA)_3(NH_3)_3$
260 K	$(IA)_6(NA)_1$
	$(IA)_6(NH_3)_1$
	$(IA)_1(NA)_3(NH_3)_3$

Table S4. The Gibbs formation free energies ΔG_{ref} (kcal mol^{-1}) of the IA–NA–NH_3 and SA–NA–NH_3 systems at the DLPNO-CCSD(T)/aug-cc-pVTZ(-PP)//ωB97X-D/6-311++G(3df,3pd) (for H, O, and N atoms) + aug-cc-pVTZ-PP with ECP28MDF (for I atom) level of theory, P = 1 atm, and T = 220 K.

Cluster		**ΔG (kcal mol^{-1})**	
		Pure-IA	**Pure-SA**
Pure-IA/SA	2	-14.41	-10.04
	3	-28.40	-19.08
	4	-49.46	-28.91
		IA–NA	**SA–NA**
IA/SA–NA	1-1	-7.57	-5.53
	1-2	-13.38	-10.15
	1-3	-18.65	-10.46
	2-1	-22.22	-15.22
	2-2	-28.50	-14.13
	3-1	-37.09	-23.12
		IA–NH_3	**SA–NH_3**
IA/SA–NH_3	1-1	-6.55	-8.93
	2-1	-24.26	-26.99
	2-2	-32.55	-36.58
	3-1	-39.94	-39.35
	3-2	-52.02	-54.77
	3-3	-51.71	-69.42
	4-1	-59.67	-48.61
	4-2	-68.49	-69.14
	5-1	-79.36	-55.71
		IA–NA–NH_3	**SA–NA–NH_3**
IA/SA–NA–NH_3	1-1-1	-15.29	-15.39
	1-1-2	-24.05	-26.65
	1-2-1	-25.46	-23.55
	1-2-2	-31.48	-33.14
	1-2-3	-46.42	-48.06

	1-3-1	-28.56	-29.19
	1-3-2	-39.04	-41.14
	2-1-1	-36.35	-32.33
	2-1-2	-46.38	-43.02
	2-1-3	-55.16	-59.66
	2-2-1	-36.46	-37.60
	2-2-2	-54.20	-55.90
	3-1-1	-44.89	-44.44
	3-1-2	-61.53	-65.15

Table S5. The total evaporation rate coefficients ($\Sigma\gamma$, s^{-1}) of SA–NA–NH_3 clusters calculated at 220 – 260 K.

Clusters	$\Sigma\gamma$ (s^{-1})		
	220 K	**240 K**	**260 K**
$(SA)_2$	5.12×10^{-1}	1.44×10^{1}	2.42×10^{2}
$(SA)_3$	1.09×10^{1}	3.12×10^{2}	5.22×10^{3}
$(SA)_4$	1.94×10^{0}	8.34×10^{1}	2.00×10^{3}
$(NA)_2$	8.37×10^{7}	4.87×10^{8}	2.20×10^{9}
$(NA)_3$	5.68×10^{11}	1.59×10^{12}	3.63×10^{12}
$(NH_3)_2$	2.01×10^{12}	2.94×10^{12}	4.12×10^{12}
$(NH_3)_3$	1.97×10^{11}	5.45×10^{11}	1.24×10^{12}
$(SA)_1(NA)_1$	6.27×10^{4}	7.16×10^{5}	5.61×10^{6}
$(SA)_1(NA)_2$	2.75×10^{5}	3.00×10^{6}	2.17×10^{7}
$(SA)_1(NA)_3$	5.73×10^{9}	2.42×10^{10}	8.18×10^{10}
$(SA)_2(NA)_1$	7.88×10^{4}	8.78×10^{5}	6.61×10^{6}
$(SA)_2(NA)_2$	1.45×10^{11}	5.57×10^{11}	1.73×10^{12}
$(SA)_3(NA)_1$	1.19×10^{6}	1.70×10^{7}	1.60×10^{8}
$(SA)_1(NH_3)_1$	3.64×10^{1}	6.19×10^{2}	6.78×10^{3}
$(SA)_2(NH_3)_1$	2.54×10^{-7}	3.05×10^{-5}	1.78×10^{-3}
$(SA)_2(NH_3)_2$	5.26×10^{0}	1.22×10^{2}	1.72×10^{3}
$(SA)_3(NH_3)_1$	5.70×10^{-3}	2.77×10^{-1}	7.12×10^{0}
$(SA)_3(NH_3)_2$	9.79×10^{-6}	8.03×10^{-4}	3.40×10^{-2}
$(SA)_3(NH_3)_3$	5.93×10^{-5}	4.20×10^{-3}	1.54×10^{-1}
$(SA)_4(NH_3)_1$	7.44×10^{0}	1.88×10^{2}	2.89×10^{3}
$(SA)_4(NH_3)_2$	6.45×10^{-5}	6.30×10^{-3}	2.98×10^{-1}
$(SA)_5(NH_3)_1$	1.12×10^{3}	3.45×10^{4}	6.26×10^{5}
$(NA)_1(NH_3)_1$	3.26×10^{4}	3.19×10^{5}	2.19×10^{6}
$(NA)_2(NH_3)_1$	3.93×10^{7}	2.39×10^{8}	1.06×10^{9}
$(NA)_2(NH_3)_2$	9.13×10^{2}	2.22×10^{4}	3.31×10^{5}
$(NA)_3(NH_3)_1$	5.30×10^{5}	5.85×10^{6}	4.53×10^{7}
$(NA)_3(NH_3)_2$	1.58×10^{2}	2.52×10^{3}	2.67×10^{4}
$(NA)_3(NH_3)_3$	2.74×10^{2}	6.19×10^{3}	8.64×10^{4}

$(NA)_4(NH_3)_1$	2.40×10^{6}	3.09×10^{7}	2.67×10^{8}
$(NA)_4(NH_3)_2$	1.69×10^{5}	2.07×10^{6}	1.72×10^{7}
$(NA)_5(NH_3)_1$	4.56×10^{6}	4.08×10^{7}	2.49×10^{8}
$(SA)_1(NA)_1(NH_3)_1$	4.02×10^{3}	6.36×10^{4}	6.68×10^{5}
$(SA)_1(NA)_1(NH_3)_2$	1.11×10^{-1}	4.11×10^{0}	8.54×10^{1}
$(SA)_1(NA)_2(NH_3)_1$	8.86×10^{1}	2.29×10^{3}	3.37×10^{4}
$(SA)_1(NA)_2(NH_3)_2$	4.25×10^{3}	1.01×10^{5}	1.46×10^{6}
$(SA)_1(NA)_2(NH_3)_3$	2.98×10^{-5}	2.47×10^{-3}	1.01×10^{-1}
$(SA)_1(NA)_3(NH_3)_1$	3.05×10^{4}	3.42×10^{5}	2.63×10^{6}
$(SA)_1(NA)_3(NH_3)_2$	1.43×10^{2}	2.41×10^{3}	2.52×10^{4}
$(SA)_2(NA)_1(NH_3)_1$	5.73×10^{4}	7.47×10^{5}	6.54×10^{6}
$(SA)_2(NA)_1(NH_3)_2$	4.87×10^{3}	1.05×10^{5}	1.41×10^{6}
$(SA)_2(NA)_1(NH_3)_3$	6.02×10^{-7}	5.48×10^{-5}	2.44×10^{-3}
$(SA)_2(NA)_2(NH_3)_1$	7.25×10^{4}	7.10×10^{5}	4.79×10^{6}
$(SA)_2(NA)_2(NH_3)_2$	2.07×10^{-3}	6.72×10^{-2}	1.25×10^{0}
$(SA)_3(NA)_1(NH_3)_1$	1.13×10^{5}	1.37×10^{6}	1.16×10^{7}
$(SA)_3(NA)_1(NH_3)_2$	6.50×10^{-1}	2.17×10^{1}	4.12×10^{2}

Table S6. Cartesian coordinates of all IA–NA–NH_3 clusters in the present study at the ωB97X-D/6-311++G(3df,3pd) (for H, O, and N atoms) + aug-cc-pVTZ-PP with ECP28MDF (for I atom) level of theory.

$(IA)_1(NA)_1(NH_3)_1$:

Atoms	X	Y	Z
N	2.915478	-0.186698	-0.059097
O	2.159906	0.697102	-0.435162
O	4.081342	-0.069885	0.167650
O	2.396832	-1.394593	0.108645
H	1.389981	-1.338087	-0.074451
I	-1.428830	-0.356142	0.026980
O	-1.283892	0.887506	-1.281094
O	-0.103788	-1.541462	-0.285673
O	-0.877765	0.584324	1.474969
H	-0.063073	2.000503	0.901473
N	0.275421	2.585119	0.097605
H	1.266500	2.391695	-0.047734
H	0.087406	3.571932	0.218204
H	-0.270162	2.156577	-0.691691

$(IA)_1(NA)_1(NH_3)_2$:

Atoms	X	Y	Z
N	3.387294	-0.110091	-0.093397
O	2.547301	-0.033475	0.892035
O	3.706174	-1.219004	-0.487385
O	3.797114	0.935511	-0.580391
H	1.833445	1.418646	0.712443
I	-1.891077	0.006567	-0.157118
O	-1.254990	1.676503	0.140329
O	-0.725236	-0.691063	-1.349123
O	-1.493821	-0.910383	1.346041
H	0.060869	-1.969062	1.082832
N	0.860706	-2.083841	0.440991
H	1.610919	-1.396423	0.705809
H	0.476606	-1.780235	-0.472568
H	1.228003	-3.026070	0.412275
N	1.316304	2.290735	0.408032
H	1.742237	2.583698	-0.465348
H	1.422586	3.023975	1.098323
H	0.289964	2.055093	0.272055

$(IA)_1(NA)_2(NH_3)_1$:

Atoms	X	Y	Z
N	3.241715	-0.839752	-0.162451
O	2.802255	-0.629110	0.960324
O	4.356798	-0.649723	-0.531189
O	2.403464	-1.348112	-1.061528
H	1.488647	-1.409317	-0.640605
N	-0.226449	2.265392	-0.690746
O	0.275395	1.067099	-0.693189
O	-1.319532	2.443594	-1.184642
O	0.440312	3.147380	-0.153926
H	1.115930	2.209279	1.273751
I	-1.371813	-0.516967	-0.133947
O	-1.248066	0.193790	1.508955
O	-0.011921	-1.680746	-0.221661
O	-2.717245	-1.844037	0.297093
H	-2.392609	-2.441838	0.980191
N	1.155148	1.429000	1.952763
H	1.373881	1.756329	2.885717
H	1.853421	0.748547	1.625839
H	0.222235	0.952681	1.915441

$(IA)_1(NA)_2(NH_3)_2$:

Atoms	X	Y	Z
N	0.917410	2.434360	-0.028051
O	0.178348	2.723457	0.933570
O	1.927359	1.722744	0.150940
O	0.622662	2.835969	-1.159607
H	-1.106815	2.358317	-1.211626
N	-2.542395	-0.905800	0.091380
O	-2.745431	0.188210	0.728303
O	-2.932696	-0.996347	-1.060778
O	-1.937322	-1.814457	0.667963
H	-1.551756	0.364451	1.930351
I	1.268487	-0.845965	-0.284205
O	1.297431	-0.970791	1.496392
O	-0.178116	0.073097	-0.752266
O	0.558797	-2.579953	-0.690012
H	-0.370244	-2.576739	-0.375193
N	-2.021701	1.876324	-1.333629
H	-1.895446	1.121385	-2.004640
H	-2.322642	1.394352	-0.454027
H	-2.737201	2.518524	-1.652151
N	-0.694771	0.612890	2.479425
H	-0.901551	0.723888	3.463424
H	0.012760	-0.127544	2.316535
H	-0.294960	1.479695	2.070274

$(IA)_1(NA)_2(NH_3)_3$:

Atoms	X	Y	Z
N	-0.231034	2.745955	-0.043725
O	-1.321880	2.578957	0.559505
O	0.834315	2.482878	0.534445
O	-0.247799	3.137619	-1.215110
H	-1.873616	2.089967	-1.681251
N	-2.603400	-1.334435	0.170184
O	-3.200014	-0.266849	0.385258
O	-2.587091	-1.838041	-0.955406
O	-1.991089	-1.884818	1.122631
H	-1.545509	-0.248433	2.082103
I	1.730297	-0.144791	-0.144545
O	1.506161	-0.377824	1.628463
O	0.021030	-0.177289	-0.750715
O	2.229387	-1.807904	-0.664004
H	0.897001	-2.707951	-0.506240
N	-2.082302	1.089141	-1.778007
H	-2.763892	0.774781	-1.068671
H	-2.397798	0.851192	-2.709248
H	-1.188981	0.590967	-1.541547
N	-0.061506	-3.169985	-0.430399
H	-0.611435	-2.765051	0.352268
H	-0.617013	-2.927729	-1.248952
H	0.007727	-4.175526	-0.333802
N	-0.936426	0.533422	2.354713
H	0.054143	0.231076	2.185652
H	-1.124770	1.356225	1.736064
H	-1.083050	0.781853	3.324590

$(IA)_1(NA)_3(NH_3)_1$:

Atoms	X	Y	Z
N	0.984744	-2.181626	-1.259174
O	0.764039	-1.132634	-1.847938
O	2.069065	-2.673025	-1.099446
O	-0.039048	-2.829127	-0.745353
H	-0.873477	-2.220338	-0.801272
N	2.179960	-0.615847	1.851665
O	1.335111	-0.129297	0.932824
O	1.753939	-0.937544	2.916920
O	3.335184	-0.672383	1.472337
H	3.376895	-0.169815	-0.319992
N	1.143410	2.747967	-0.456310
O	0.416052	3.358438	0.266036
O	2.359461	2.837406	-0.508825
O	0.626292	1.868825	-1.315148
H	-0.370304	1.713061	-1.082507
I	-2.358084	0.044142	0.245444
O	-2.159644	-1.481016	-0.699873
O	-1.784748	1.350252	-0.860219
O	-1.086643	-0.062622	1.527458
H	0.357732	-0.142587	1.281932
N	3.188608	0.243886	-1.248048
H	3.965639	0.084844	-1.878108
H	2.329089	-0.196969	-1.617962
H	3.003328	1.253438	-1.117771

$(IA)_1(NA)_3(NH_3)_2$:

Atoms	X	Y	Z
N	0.405580	-1.885811	-1.678967
O	0.186390	-0.712847	-1.886186
O	1.441022	-2.464578	-1.927473
O	-0.539936	-2.618843	-1.141189
H	-1.348464	-2.000233	-0.900412
N	1.826048	-1.045045	2.011372
O	1.216270	-0.621436	0.891421
O	1.242408	-0.964030	3.047822
O	2.942129	-1.486224	1.829497
H	3.524499	-1.106320	0.115285
N	2.686540	2.030661	-0.076821
O	3.495505	1.656298	0.753017
O	2.703532	1.527608	-1.248033
O	1.822653	2.886531	0.178570
H	-0.975438	1.976172	-1.345894
I	-2.646376	0.232467	0.424257
O	-2.561975	-1.343399	-0.462062
O	-2.482507	1.490405	-0.853598
O	-1.085326	0.343420	1.320200
H	0.291342	-0.261328	1.133772
N	3.653741	-0.916086	-0.889983
H	4.618327	-1.070135	-1.155918
H	3.022433	-1.528165	-1.416469
H	3.367841	0.096216	-1.066417
N	-0.029778	2.251403	-1.708308
H	0.445653	1.423454	-2.063912
H	0.595968	2.625749	-0.952398
H	-0.120459	2.934773	-2.450174

$(IA)_2(NA)_1(NH_3)_1$:

Atoms	X	Y	Z
N	-2.625495	1.689453	-0.678585
O	-2.213277	2.753768	-0.210411
O	-2.852164	1.508431	-1.847922
O	-2.815449	0.719984	0.170289
H	-1.365475	2.264776	1.290985
I	-1.420240	-1.144816	-0.022772
O	-1.293550	-0.951201	1.745383
O	-0.246137	0.071177	-0.703035
O	-0.256684	-2.654603	-0.226248
H	0.652551	-2.381532	0.033523
I	2.102504	0.297093	-0.316848
O	2.096343	-1.364700	0.341769
O	1.765753	1.368211	1.075661
O	4.029799	0.501681	-0.325985
H	4.404610	0.082665	0.457711
N	-0.778782	1.805458	2.016800
H	-0.824322	2.306806	2.894961
H	0.203419	1.737328	1.676842
H	-1.117865	0.832944	2.122337

$(IA)_2(NA)_1(NH_3)_2$:

Atoms	X	Y	Z
N	2.904083	1.698666	0.132322
O	2.083109	2.466318	0.738890
O	3.197588	1.938837	-1.028755
O	3.352356	0.721437	0.743864
H	1.293027	1.453556	1.901499
I	-2.567497	0.193527	0.003358
O	-1.630242	-1.336609	-0.328821
O	-1.899533	0.855192	1.538807
O	-2.067167	1.389579	-1.249955
H	-0.569497	2.161046	-1.279823
I	0.814317	-1.546938	-0.325249
O	0.816180	-1.730110	1.454433
O	0.702205	0.208783	-0.615330
O	2.706512	-1.687313	-0.638634
H	3.139418	-0.893880	-0.255932
N	0.347520	2.654832	-1.416027
H	0.223653	3.565185	-1.841371
H	0.939910	2.066221	-1.997538
H	0.874800	2.733626	-0.519578
N	0.681335	0.824642	2.466227
H	0.777563	1.018693	3.454483
H	0.927833	-0.160045	2.249806
H	-0.306798	0.930480	2.155061

$(IA)_2(NA)_1(NH_3)_3$:

Atoms	X	Y	Z
N	-2.226050	2.522677	0.186169
O	-1.119380	3.014940	0.579678
O	-2.805461	1.711519	0.927850
O	-2.663648	2.830942	-0.910575
H	-0.177891	2.837469	-1.019260
I	3.225204	-0.038694	-0.003587
O	2.519635	-1.503240	-0.789590
O	2.660935	1.358361	-0.992399
O	2.304422	0.080868	1.545371
H	0.797072	0.767322	1.968816
I	-2.398287	-0.933157	-0.159285
O	-1.600107	-1.174570	1.465724
O	-1.077593	-0.059341	-1.023855
O	-2.217734	-2.585960	-0.855613
H	-0.437068	-2.935992	-0.486344
N	0.351350	-2.798923	0.176281
H	0.682808	-3.688384	0.528677
H	-0.078200	-2.245758	0.935368
H	1.147131	-2.257851	-0.248478
N	-0.168577	1.028626	2.254530
H	-0.511060	1.847192	1.706201
H	-0.200403	1.240856	3.243589
H	-0.796002	0.220951	2.038112
N	0.173893	2.180244	-1.732023
H	0.099479	2.579729	-2.658136
H	-0.427181	1.331825	-1.638035
H	1.151841	1.894218	-1.505714

$(IA)_2(NA)_2(NH_3)_1$:

Atoms	X	Y	Z
N	2.103338	-2.450728	1.062798
O	3.029829	-1.739059	0.737903
O	1.743690	-2.688274	2.182795
O	1.399456	-3.033183	0.087572
H	1.529600	-2.462142	-0.731386
N	0.669854	2.750928	0.755536
O	1.906318	2.881694	0.917164
O	0.205304	2.751567	-0.396535
O	-0.064583	2.563033	1.732568
H	2.350135	1.540279	2.103996
I	-2.293101	-0.500162	0.300152
O	-4.016643	-0.753986	0.038727
O	-1.612706	-0.271663	-1.370647
O	-2.393027	1.291017	0.934641
H	-1.520534	1.710466	1.138883
I	0.751142	0.247378	-1.358902
O	1.309522	-1.353771	-1.911707
O	0.419842	-0.065018	0.405496
O	2.524377	0.955614	-1.075129
H	2.453867	1.830912	-0.646232
N	2.210426	0.537915	2.318062
H	1.925869	0.400247	3.280409
H	3.031775	-0.025043	2.098534
H	1.456736	0.232223	1.651964

$(IA)_2(NA)_2(NH_3)_2$:

Atoms	X	Y	Z
N	3.487066	-0.631799	1.239746
O	3.453231	-1.488469	0.346679
O	4.141118	0.414289	1.089463
O	2.827798	-0.798504	2.291137
H	1.512358	-1.889632	1.863016
N	-0.167701	3.073128	-0.281086
O	-0.692866	2.870446	0.926848
O	-0.741701	2.628548	-1.240496
O	0.869719	3.696343	-0.284511
H	1.936480	2.894626	1.337325
I	0.586069	-0.411621	-1.460778
O	0.641682	-2.183089	-1.246867
O	0.628565	0.219072	0.225752
O	2.438569	-0.123879	-1.867652
H	2.996394	-0.597341	-1.211892
I	-2.744491	-0.490052	0.411716
O	-1.786474	-0.543126	-1.136344
O	-1.843973	-1.519871	1.575105
O	-2.557511	1.197214	1.020941
H	-1.440749	2.165922	0.845840
N	2.040465	1.968400	1.751600
H	3.009406	1.593183	1.667175
H	1.441078	1.311780	1.202577
H	1.741587	1.968902	2.718928
N	0.743612	-2.493063	1.505238
H	-0.185253	-2.047833	1.642630
H	0.772761	-3.403134	1.947535
H	0.862945	-2.576243	0.478244

$(IA)_2(NA)_3(NH_3)_1$:

Atoms	X	Y	Z
N	-3.474957	0.628776	-0.976909
O	-2.306535	0.978580	-0.911754
O	-4.415615	1.333896	-1.159676
O	-3.728264	-0.671123	-0.839671
H	-2.849505	-1.130097	-0.658152
N	-1.998756	-1.061183	2.545963
O	-0.829180	-1.241918	2.844247
O	-2.896504	-1.817453	2.711005
O	-2.326402	0.117441	1.993598
H	-1.492129	0.628749	1.802753
N	4.108135	-0.718460	0.104806
O	3.821520	-0.474747	1.268615
O	4.737540	-1.652807	-0.279991
O	3.698124	0.136169	-0.828568
H	3.086734	0.819469	-0.396377
N	1.565148	0.270703	2.757968
H	2.320629	0.057213	2.089154
H	1.946405	0.467962	3.675549
H	1.008921	1.065019	2.385785
I	0.331745	1.779471	-0.288524
O	2.092620	1.945300	0.040625
O	-0.300502	1.748632	1.406665
O	0.034037	3.668275	-0.564970
H	0.477284	4.188783	0.114415
I	0.053744	-1.845219	-0.961764
O	0.747424	-0.470160	0.072425
O	-1.600313	-2.038742	-0.279699
O	-0.130450	-1.054905	-2.543627
H	0.893761	-0.502811	2.795502

$(IA)_3(NA)_1(NH_3)_1$:

Atoms	X	Y	Z
N	-0.302532	3.087877	-1.128785
O	-0.030972	2.619907	-0.042589
O	-1.218594	2.437396	-1.862345
O	0.148610	4.074455	-1.621876
I	3.605863	0.170217	0.520747
O	3.302569	-1.566446	0.232991
O	2.817548	0.987406	-0.987827
O	2.566836	0.685481	1.869712
H	0.042024	0.202109	1.782081
I	-3.487672	0.027151	0.399087
O	-3.394931	-1.708207	0.786081
O	-2.920253	0.935435	1.846557
O	-2.061520	0.187115	-0.768718
H	-1.451678	1.600027	-1.368619
I	-0.224388	-1.495554	-0.832964
O	0.030146	-1.215120	0.909843
O	0.591733	-0.133698	-1.669657
O	1.151712	-2.808317	-1.047440
H	1.959724	-2.480097	-0.595691
H	1.939119	0.546919	-1.225245
N	-0.232384	1.057487	2.312176
H	0.186712	1.855118	1.842129
H	0.107076	0.991832	3.263292
H	-1.273237	1.107143	2.256378

$(IA)_3(NA)_1(NH_3)_2$:

Atoms	X	Y	Z
N	0.749358	2.365446	1.800145
O	-0.335725	2.845911	1.441800
O	1.759541	2.561485	1.076481
O	0.836568	1.698750	2.831030
H	-0.904812	1.051338	2.862547
I	-3.670478	0.318301	-0.851790
O	-3.164674	-1.359524	-0.409330
O	-3.310417	1.280067	0.630604
O	-2.443749	0.880267	-2.048259
H	-1.010489	1.610316	-1.564779
I	3.569665	0.103307	-0.891416
O	2.793380	-1.494188	-0.706072
O	2.446725	1.143400	-1.808715
O	3.516417	0.778804	0.861116
H	2.764823	1.469537	1.023934
I	0.274559	-1.841522	0.644309
O	0.218590	-0.085876	0.335982
O	-0.688848	-2.008877	2.147642
O	-0.891859	-2.510307	-0.676622
H	-1.786628	-2.031564	-0.623380
N	-1.763168	0.490561	2.739159
H	-1.474569	-0.495243	2.586155
H	-2.287007	0.823003	1.896272
H	-2.353770	0.569047	3.557666
N	-0.177853	2.185186	-1.297805
H	-0.290618	2.513448	-0.322377
H	-0.099748	2.984923	-1.914367
H	0.688310	1.632970	-1.355842

$(IA)_3(NA)_2(NH_3)_1$:

Atoms	X	Y	Z
N	-0.870445	-1.748378	-2.318798
O	-1.406140	-1.966133	-1.181800
O	0.334003	-1.883719	-2.470815
O	-1.621788	-1.422910	-3.240613
H	-3.151945	-0.975903	-2.244197
N	0.904346	1.603534	2.697389
O	1.167452	0.481237	3.075939
O	0.064359	2.335534	3.124621
O	1.622613	2.093935	1.671977
H	2.223794	1.363424	1.293655
I	2.317938	-0.762230	-0.633437
O	1.253676	-1.513280	0.584125
O	3.112614	0.528042	0.330148
O	3.761592	-2.044064	-0.537370
H	4.024757	-2.170592	0.382328
I	-1.341094	-1.342672	1.226922
O	-3.109373	-1.466595	1.087750
O	-1.086886	0.426105	0.879025
O	-1.276319	-1.099363	3.133291
H	-0.495467	-0.562248	3.361204
I	-0.544250	2.063770	-0.645443
O	-2.055346	1.769521	-1.548511
O	0.627263	0.905066	-1.372072
O	0.034966	3.581352	-1.693575
H	0.060110	3.350961	-2.629754
N	-3.681764	-0.418763	-1.550060
H	-3.644702	-0.903222	-0.638314
H	-4.635802	-0.251661	-1.844434
H	-3.154656	0.476676	-1.463388

$(IA)_4(NA)_1(NH_3)_1$:

Atoms	X	Y	Z
N	-3.817829	-1.658823	1.459851
O	-3.868573	-0.360482	1.536259
O	-4.504810	-2.233114	0.651476
O	-3.038264	-2.224126	2.229980
H	-1.824126	-0.915462	2.603334
I	0.992561	2.416697	-0.150962
O	0.129236	1.405032	-1.363849
O	0.867228	1.572603	1.427210
O	-0.448090	3.628675	0.141438
H	-1.246617	3.095547	0.376175
I	3.434293	-0.496945	0.285563
O	5.185190	-0.336715	0.379425
O	2.877163	1.013766	-0.565433
O	2.971164	0.037946	2.054938
H	2.171840	0.616387	1.958875
I	0.074295	-2.324062	-0.746623
O	0.706834	-1.458718	0.708368
O	1.289488	-3.573818	-1.041414
O	0.693655	-1.094035	-2.061940
H	0.458709	-0.163355	-1.807239
I	-3.151801	0.704747	-0.416298
O	-2.347745	1.787471	0.780801
O	-2.053852	-0.702358	-0.564560
O	-2.556896	1.638846	-1.988430
H	-1.580204	1.687307	-1.956725
N	-1.072625	-0.213746	2.472989
H	-0.631678	0.033084	3.350483
H	-0.365784	-0.601696	1.818892
H	-1.478228	0.625208	2.033167

Table S7. Structural *RMSD* (in Å) and Gibbs free energy (in kcal mol^{-1}) comparisons of $(IA)_1(NA)_1$, $(IA)_1(NH_3)_1$, and $(IA)_1(NA)_1(NH_3)_1$ clusters at different levels of theory.

Clusters	*RMSD*	$\Delta G_{\text{DLPNO-CCSD(T)}}$[1]	$\Delta G_{\text{DLPNO-CCSD(T)}}$[2]	$\Delta\Delta G_{\text{DLPNO-CCSD(T)}}$	$\Delta G_{\text{CCSD(T)}}$
$(IA)_1(NA)_1$	0.005	-4.90	-4.42	0.50	-4.92
$(IA)_1(NH_3)_1$	0.004	-3.85	-3.12	0.73	-3.79
$(IA)_1(NA)_1(NH_3)_1$	0.023	-9.23	-9.06	0.17	-9.78

RMSD is the structural differences of the clusters optimized at the *ω*B97X-D/6-311++G(3df,3pd) (for H, O, and N atoms) + aug-cc-pVTZ-PP (for I atom) and *ω*B97X-D/ aug-cc-pVTZ (for H, O, and N atoms) + aug-cc-pVTZ-PP (for I atom) levels of theory. [1] $\Delta G_{\text{DLPNO-CCSD(T)}}$ is the Gibbs free energy calculated at the DLPNO-CCSD(T)/ aug-cc-pVTZ(-PP)//*ω*B97X-D/6-311++G(3df,3pd) (for H, O, and N atoms) + aug-cc-pVTZ-PP (for I atom) level of theory. [2] $\Delta G_{\text{DLPNO-CCSD(T)}}$ is the Gibbs free energy calculated at the DLPNO-CCSD(T)/aug-cc-pVTZ(-PP)//*ω*B97X-D/aug-cc-pVTZ (for H, O, and N atoms) + aug-cc-pVTZ-PP (for I atom) level of theory. $\Delta\Delta G_{\text{DLPNO-CCSD(T)}}$ is the energy differences between the two basis sets. $\Delta G_{\text{CCSD(T)}}$ is the energy calculated at the CCSD(T)/aug-cc-pVTZ(-PP)//*ω*B97X-D/6-311++G(3df,3pd) (for H, O, and N atoms) + aug-cc-pVTZ-PP (for I atom) level of theory.

Supplementary Reference

Bork, N., Elm, J., Olenius, T. and Vehkamäki, H.: Methane sulfonic acid-enhanced formation of molecular clusters of sulfuric acid and dimethyl amine, Atmos. Chem. Phys., 14, 12023–12030, http://doi.org/10.5194/acp-14-12023-2014, 2014.

Elm, J. and Kristensen, K.: Basis set convergence of the binding energies of strongly hydrogen-bonded atmospheric clusters, Phys. Chem. Chem. Phys., 19, 1122–1133, http://doi.org/10.1039/c6cp06851k, 2017.

Francl, M. M., Pietro, W. J., Hehre, W. J., Binkley, J. S., Gordon, M. S., DeFrees, D. J. and Pople, J. A.: Self-consistent molecular orbital methods. XXIII. A polarization-type basis set for second-row elements, J. Chem. Phys. , 77, 3654–3665, http://doi.org/10.1063/1.444267, 1982.

Frisch, M. J., Trucks, G. W., Schlegel, H. B., Scuseria, G. E., Robb, M. A., Cheeseman, J. R., Scalmani, G., Barone, V., Mennucci, B., Petersson, G. A., Nakatsuji, H., Caricato, M., Li, X., Hratchian, H. P., Izmaylov, A. F., Bloino, J., Zheng, G., Sonnenberg, J. L., Hada, M., Ehara, M., Toyota, K., Fukuda, R., Hasegawa, J., Ishida, M., Nakajima, T., Honda, Y., Kitao, O., Nakai, H., Vreven, T., Montgomery, J. A., Peralta, J. E., Ogliaro, F., Bearpark, M., Heyd, J. J., Brothers, E., Kudin, K. N., Staroverov, V. N., Kobayashi, R., Normand, J., Raghavachari, K., Rendell, A., Burant, J. C., Iyengar, S. S., Tomasi, J., Cossi, M., Rega, N., Millam, J. M., Klene, M., Knox, J. E., Cross, J. B., Bakken, V., Adamo, C., Jaramillo, J., Gomperts, R., Stratmann, R. E., Yazyev, O., Austin, A. J., Cammi, R., Pomelli, C., Ochterski, J. W., Martin, R. L., Morokuma, K., Zakrzewski, V. G., Voth, G. A., Salvador, P., Dannenberg, J. J., Dapprich, S., Daniels, A. D., Farkas, O., Foresman, J. B., Ortiz, J. V., Cioslowski, J. and Fox, D. J.: Gaussian 16, Revision A.03, Gaussian Inc, Wallingford CT, 2016.

Lu, T. and Chen, F.: Multiwfn: a multifunctional wavefunction analyzer, J. Comput. Chem., 33, 580–592, http://doi.org/10.1002/jcc.22885, 2012.

Peterson, K. A., Figgen, D., Goll, E., Stoll, H. and Dolg, M.: Systematically convergent basis sets with relativistic pseudopotentials. II. Small-core pseudopotentials and correlation consistent basis sets for the post-d group 16–18 elements, J. Chem. Phys. , 119, 11113–11123, http://doi.org/10.1063/1.1622924, 2003.

Rappé, A. K., Casewit, C. J., Colwell, K. S., Goddard, W. A. and Skif, W. M.: UFF, a full periodic table force field for molecular mechanics and molecular dynamics simulations, J. Am. Chem. Soc., 114, 10024–10035, http://doi.org/10.1021/ja00051a040, 1992.

Stewart, J. J.: Optimization of parameters for semiempirical methods VI: more modifications to the NDDO approximations and re-optimization of parameters, J. Mol. Model., 19, 1–32, http://doi.org/10.1007/s00894-012-1667-x, 2013.

Stewart, J. J. P.: MOPAC2016, Colorado Springs, CO (USA), http://openmopac.net/MOPAC2016.html (last access: 2022 Feb 2024), 2016.

Zhang, J. and Dolg, M.: ABCluster: the artificial bee colony algorithm for cluster global optimization, Phys. Chem. Chem. Phys., 17, 24173–24181, http://doi.org/10.1039/c5cp04060d, 2015.